Finite-size effect on magnetic properties in iron sulfide nanowire arrays

2008 Nanotechnology 19 195706

(http://iopscience.iop.org/0957-4484/19/19/195706)

Nanotechnology **19** (2008) 195706 (5pp) doi:10.1088/0957-4484/19/19/195706

Finite-size effect on magnetic properties in iron sulfide nanowire arrays

G H Yue[1,3], P X Yan[2], L S Wang[1], W Wang[1], Y Z Chen[1] and D L Peng[1,3]

[1] Department of Materials Science and Engineering, Research Center of Materials Design and Applications, Xiamen University, Xiamen 361005, People's Republic of China
[2] School of Physical Science and Technology, Lanzhou University, Lanzhou 730000, People's Republic of China

E-mail: yuegh@126.com and dlpeng@xmu.edu.cn

Received 19 December 2007, in final form 28 February 2008
Published 8 April 2008
Online at stacks.iop.org/Nano/19/195706

Abstract

We report the size effect on the magnetic properties in Fe_7S_8 nanowire arrays. Samples with diameters in the range of 50–200 nm have been prepared by electrodeposition with AAO films. The Mössbauer measurement results show that four parameters (hyperfine fields, isomer shift, quadrupole splitting, full width at half-maximum) increased with decreasing the diameter of the nanowires. The magnetic properties were investigated. The hysteresis loop shape and the magnetization are dependent on the diameter of the nanowires. The thermomagnetic measurements on the as-synthesized nanowire samples and the corresponding bulk display a mixed-type curve and a Weiss-type curve, respectively.

In recent years, there have been a considerable number of studies regarding magnetic nanowire arrays embedded in anodic aluminum oxide (AAO) templates [1–6], which may have a strong potential as possible candidates for a future generation of high-density magnetic information storage media [3]. Investigations to date have included their structural [1, 3], magnetic [1–3, 7–9], optical [4] and magneto-optical [5, 10] properties. Magnetic metal nanowires, such as Fe [11], Co [12], Ni [13] and their alloys [14], have been prepared and studied successfully. Although there are many reports of nanowires of several metal chalcogenides [1, 3, 6], oxides [15] and nitrides [16], there are few reports to date on iron sulfide nanowires, possibly because of the inherent difficulty in the synthesis and control of stoichiometry of these materials. The Fe–S system has a complex phase diagram and a broad range of compositions of $Fe_{1-x}S$ (pyrrhotite) phases [17] occurring between FeS and FeS_2, showing interesting magnetic [18] and electrical properties [19]. The pyrrhotite Fe_7S_8, with monoclinic, trigonal and hexagonal structures, has been extensively studied due to its interesting ferromagnetic properties [3, 20] and complex crystalline structure [18]. Iron chalcogenides were synthesized by the elemental reaction in evacuated tubes at elevated temperature [21, 22], or obtained by the method of rapidly quenched ternary, the hydrothermal reduction route [23–25], the simple flux method [26–28] or pulsed electrodeposition in the AAO template [3]. In our previous study [3], we successfully obtained Fe_7S_8 nanowire arrays using an improved method, and studied their structure and magnetic properties.

In this work, the iron sulfide (Fe_7S_8) nanowire arrays with pyrrhotite nanostructures and diameters of 50, 100, 150 and 200 nm were prepared, and their magnetic properties relative to the finite-size effect were investigated.

The highly ordered porous anodic aluminum oxide (AAO) films were generated by anodizing an aluminum foil (99.999%) in an acid solution using a two-step anodizing process: (1) the high purity aluminum foils were electropolished in a 1:3 volume mixture of $HClO_4$ and C_2H_5OH; (2) the polished aluminum foils were anodized in 0.4 M oxalic or 0.6 M phosphoric acid solution at $40V_{DC}$ or $90V_{DC}$ at a temperature lower than 10 °C, respectively. The latter process contained the following four steps: (1) the polished aluminum foil was anodized for 30 min to eliminate large ridges and to 'texture' the aluminum foil surface; (2) the oxide film was dissolved away in a mixed solution of 0.1 M H_2CrO_4 and 0.2 M H_3PO_4 at 60 °C for 10 min; (3) the aluminum foil was rinsed with deionized water, then anodized at the same conditions for 1–5 h, to create long range order; (4) with the oxide film removed,

[3] Authors to whom any correspondence should be addressed.

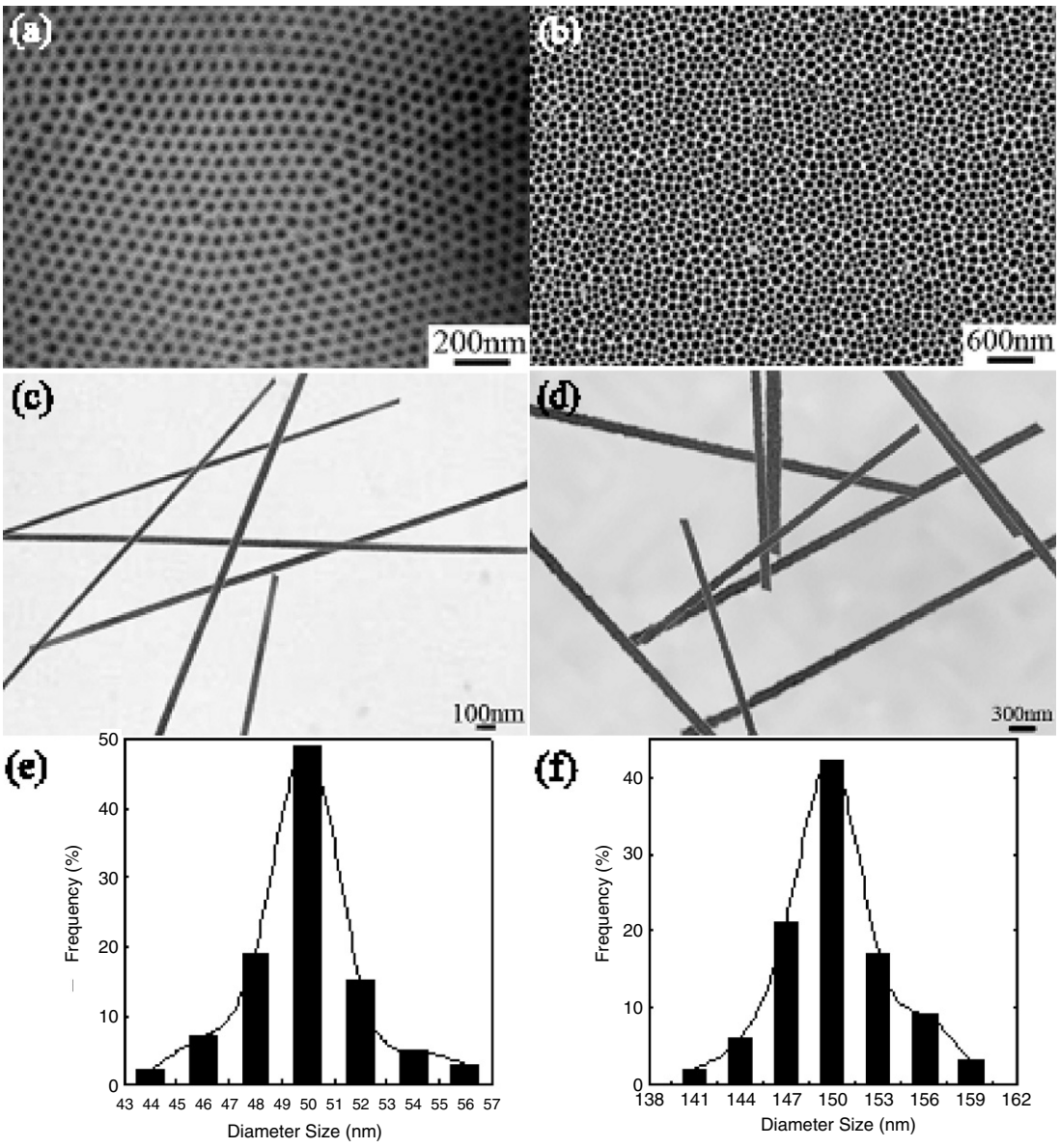

Figure 1. (a) and (b) SEM images of anodic aluminum oxide templates obtained by anodizing in oxalic and phosphoric acid solution. (c) and (d) TEM images of the Fe_7S_8 nanowires with diameters of 50 and 150 nm. (e) and (f) Diameter distributions of the nanowires with diameters of 50 and 150 nm, respectively.

the aluminum foil was further anodized for 1 h. In this way, an aluminum oxide template with highly ordered pores was formed. The aluminum oxide templates with pore diameters ranging from several tens to hundreds of nanometers were achieved by adjusting the height of the voltage in different types of anodizing solution such as sulfuric and phosphoric acid. The anodization time was determined by the required thickness of the anodic aluminum oxide templates.

Structural characterization of the Fe_7S_8 nanowires was performed by means of x-ray diffraction using a Rigaku/Max-2400 diffractometer with Cu Kα radiation. Transmission electron microscopy (TEM) and selected-area electron diffraction (SAED) were performed by using a JEO 20003 microscope which operated at 75–100 kV. Scanning electron microscopy (SEM) was operated by using a JSM-5600 microscope. The micro-magnetic and macro-magnetic properties of the nanowire arrays at room temperature (RT) were characterized using a Mössbauer spectrometer in a constant acceleration spectrometer with a source of ^{57}Co in rhodium. The RT spectra were fitted by a hyperfine field distribution (HFD). The isomer shifts were determined relative to α-Fe at RT. Magnetic property measurements (300–650 K) were made using a vibrating sample magnetometer (VSM).

The Fe_7S_8 nanowires were electrodeposited into nanometer-size cylindrical pores in aluminum anodic oxide films. They are typically 4 μm in length, arrayed in a parallel manner. Detailed electrodeposited conditions of the Fe_7S_8 nanowires have been published in our earlier work [3]. Figures 1(a) and (b) show the SEM images of anodic aluminum oxide templates obtained by anodizing in oxalic and phosphoric acid solution in a two-step process, respectively. It was found that the nanopores are uniform and highly ordered with average

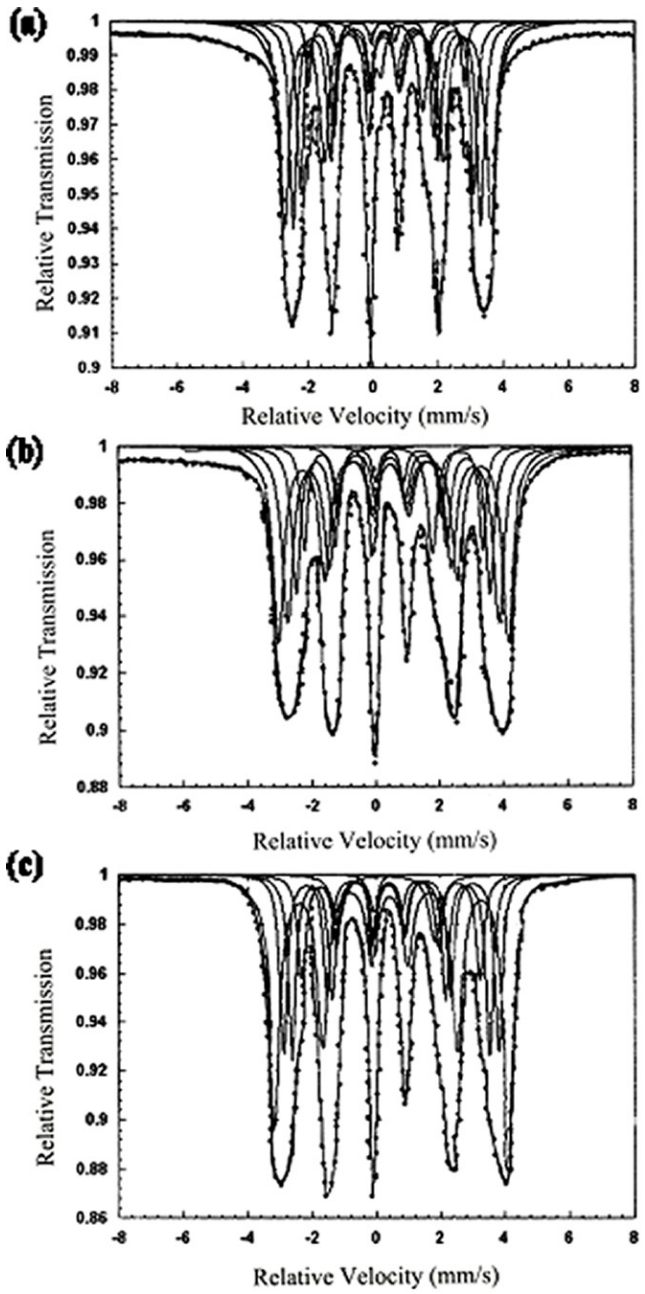

Figure 2. The Mössbauer spectra of Fe_7S_8 bulk (a) and Fe_7S_8 nanowire arrays with diameters of 50 (b) and 150 nm (c) obtained at room temperature.

diameters of 50 ± 4 nm and 150 ± 9 nm, respectively. In addition, the varied lengths of the nanopores can be achieved by adjusting the anodizing time. Figures 1(c) and (d) show the TEM images of Fe_7S_8 nanowires with diameters of 50 ± 4 nm and 150 ± 9 nm, respectively, which were obtained by electrodeposition in the anodic aluminum templates. The diameter distributions of the nanowires are shown in figures 1(e) and (f), respectively. The lengths of these nanowires could be varied by controlling the electrodeposition time. Our previous work [3] showed that nanowires were continuous and highly crystalline with a monoclinic pyrrhotite structure. The above results indicate that the Fe_7S_8 nanowire may be an excellent candidate as a good quasi-one-dimensional nanomagnet for the application study of the one-dimensional magnetic system.

Table 1. The hyperfine parameters of pyrrhotite Fe_7S_8 bulk and Fe_7S_8 nanowire arrays.

	HF (T)	IS (mm s^{-1})	QS (mm s^{-1})	FWHM (mm s^{-1})	Intensity (%)
Bulk	0	1.12	2.73	0.32	11.45
	0	1.03	1.55	0.21	12.69
	27.48	0.67	0.03	0.41	22.91
	25.09	0.71	0.02	0.43	18.81
	23.26	0.68	0.03	0.45	16.19
	21.05	0.69	0.02	0.21	11.36
200 nm	0	1.13	2.76	0.37	11.62
	0	1.05	1.58	0.25	12.83
	28.01	0.73	0.04	0.48	23.17
	25.11	0.75	0.03	0.51	18.95
	23.24	0.72	0.04	0.49	16.32
	21.08	0.71	0.02	0.23	11.39
150 nm	0	1.16	2.81	0.41	11.73
	0	1.09	1.61	0.27	13.01
	28.03	0.78	0.05	0.51	23.25
	25.13	0.81	0.03	0.57	19.07
	23.29	0.73	0.04	0.53	16.59
	21.04	0.71	0.03	0.27	11.42
100 nm	0	1.17	2.82	0.49	12.15
	0	1.12	1.64	0.31	13.41
	28.06	0.79	0.07	0.55	23.37
	25.17	0.83	0.05	0.63	19.21
	23.29	0.73	0.06	0.59	16.73
	21.13	0.73	0.04	0.32	11.61
50 nm	0	1.22	2.85	0.59	12.36
	0	1.15	1.67	0.37	13.59
	28.17	0.81	0.11	0.73	23.51
	25.25	0.83	0.09	0.81	19.38
	23.37	0.75	0.08	0.67	16.97
	21.19	0.76	0.05	0.45	11.86

Room temperature ^{57}Fe Mössbauer spectra were measured for arrays of the Fe_7S_8 nanowires within the supporting anodic aluminum oxide templates, with a γ-ray beam perpendicular to the anodic aluminum oxide template film (namely, the γ-ray beam parallel to the Fe_7S_8 nanowire arrays). Figure 2 shows the Mössbauer spectra of Fe_7S_8 bulk and Fe_7S_8 nanowire arrays with diameters of 50 and 150 nm obtained at room temperatures. The six-line pattern of the Mössbauer spectra was fitted with four sextets, and the spectrum studies of the single crystals of Fe_7S_8 have shown that monoclinic pyrrhotite has four equivalent Fe sites [29]. Two Fe sites, Fe-1 and Fe-3, occur together in the same layers, and the other two Fe sites, Fe-2 and Fe-4, occur together along with vacancies. The room temperature hyperfine fields are 30.0, 29.5, 25.3 and 22.8 T in the intensity ratios 2:1:2:2, corresponding to the four Fe sites (Fe-1, Fe-2, Fe-3 and Fe-4), respectively [29].

The hyperfine parameters of monoclinic pyrrhotite of Fe_7S_8 nanowires found in this study (table 1) are in good agreement with [29] and [30]. The observed hyperfine fields (HF), isomer shift (IS), quadrupole splitting (QS), full width at half-maximum (FWHM) and relative intensity of Mössbauer spectra increase as the diameter of nanowires decreases. The relative intensity and IS change a little, whereas the FWHM and QS values have an obvious change. Some

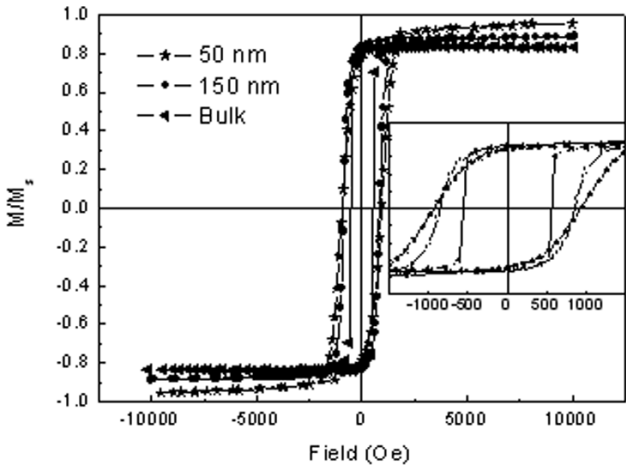

Figure 3. Normalized hysteresis loops at 300 K of Fe_7S_8 nanowire arrays with diameters of 50 and 150 nm, and Fe_7S_8 bulk.

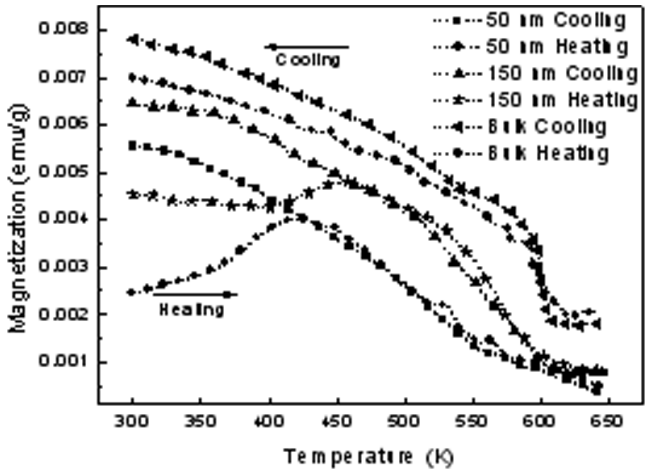

Figure 4. Temperature dependence of magnetization between 300 and 650 K of the Fe_7S_8 nanowire arrays with diameters of 50 and 150 nm, and Fe_7S_8 bulk.

important information can be obtained from the hyperfine parameters. The relative intensity and IS results indicate that the composition of Fe_7S_8 nanowires remains the same as the diameters of nanowires decrease with respect to Fe_7S_8 bulk. The FWHM and QS of the iron sulfide nanowires show surface-related contributions due to changes in the local symmetry, and in the nanowires the increasing contribution from iron at sites of reduced local symmetry, i.e. from the surface or the near-surface region to the overall spectrum. Therefore, the FWHM and QS results show that the symmetry environment of iron ions in nanowires decreases as the diameter of the nanowires decreases with respect to that of Fe_7S_8 bulk. This results from the increased relative intensity of iron ions in the surface with disorder status as the Fe_7S_8 bulk changes into nanowires.

The hysteresis loops of Fe_7S_8 nanowires with a diameter of 50 and 150 nm at 300 K (figure 3) show that the magnetization clearly traces a hysteretic curve like that of Fe_7S_8 bulk, saturating rapidly at about 2500 Oe with a strong coercive field. It is also found that the hysteresis loop shape for the nanowire shifts from a rectangular shape to a parallelogram shape as the diameters of the nanowires decrease, indicating that the magnetic exchange interaction between Fe^{3+} ions in Fe_7S_8 nanowires become weaker. It was also found that the lattice constant changes very little with changing the diameter of the nanowires [3]. The remnant magnetization is 0.78, 0.84 and 0.80 and the coercivity is 562.22, 931.33 and 854.61 Oe of the Fe_7S_8 bulk and the nanowires with diameters of 50 and 150 nm, respectively. The lower hysteresis loop indicates the predominant ferromagnetic interactions, and the out-of-plane hysteresis loop shows that they (the Fe_7S_8 bulk and the nanowires with diameters of 50 and 150 nm) have a better square ratio of about 0.90, 0.84 and 0.80, respectively.

The magnetic behaviors of the non-stoichiometric pyrrhotite ($Fe_{0.87}S$–$Fe_{0.92}S$) were categorized according to the following three types [31]: (1) Weiss type; (2) peak type: in this case the magnetization is characterized by an abrupt rise and fall of a ferrimagnetic peak in a narrow temperature range while elsewhere the pyrrhotite is antiferromagnetic; (3) mixed type: the pyrrhotite for this magnetic type is actually a mixture of Weiss-type and peak-type pyrrhotite, and hence the thermomagnetic behavior is a combination of the first two types. In our experiment, the Weiss-type and the mixed-type curve were found in the thermomagnetic properties measurements. The results of thermomagnetic measurements on the synthesized nanowire samples and the bulk are shown in figure 4. The magnetization decreases as the diameter of the nanowires decreases. In addition, the bulk sample displays a Weiss-type curve, whereas the nanowire samples exhibit a mixed-type curve. In the temperature range between 300 and 650 K, the thermomagnetic behavior for all the samples can be reversed upon changing from heating to cooling. The magnetization in Weiss-type pyrrhotite of the bulk sample is recovered with a hysteresis of 10–20 K upon cooling. In the nanowire samples, a λ-shaped peak is reversed on the cooling ramp, but is accompanied by the production of a Weiss-type component, indicating that the peak type has been partially converted into Weiss type at high temperature. On the other hand, this means that the heating mixed-type gives rise to an increase of the Weiss-type component and a decrease of the peak-type component. This change can be attributed to the decomposition of samples: at the highest experimental temperatures sulfur may evolve from the pyrrhotite samples so that the stoichiometry of the samples, and accordingly the magnetic properties, are altered. This feature suggests that the peak-type pyrrhotite has the same structure as the high temperature form of the Weiss-type, and that this structure is maintained, at least in part, when a relatively fast cooling is performed. We know that the magnetic structure determines the magnetic properties, which is associated with each of the four crystallographically distinct iron sites and indicates the Fe_7S_8 as an ionic species which corresponds to a configuration of $(Fe_2^{3+}Fe^{2+})[Fe_4^{2+}]S_8$ in which Fe^{3+} ions are confined to the vacancy layers [32]. Accordingly, excess iron vacancies yield a net ferrimagnetism in the 4*C* structure nanowires and the magnetic configuration consisting of ferromagnetic coupling within the iron layers and antiferromagnetic coupling between the layers.

In summary, we have fabricated Fe_7S_8 nanowire arrays with diameters in the range of 50–200 nm by an electrodepositing technology with two-step anodizing anodic aluminum oxide films, and measured their magnetic properties. The hysteresis loop shape and the magnetization change with the diameter of the nanowires. The thermomagnetic measurements on the as-synthesized samples and the bulk display a mixed-type curve and a Weiss-type curve, respectively. In the temperature range between 300 and 650 K, the thermomagnetic behavior for all the samples can be reversed upon the change from heating to cooling. In light of our results, it seems that the Fe_7S_8 nanowire array can be a promising candidate as a good quasi-one-dimensional nanomagnet for the study of the one-dimensional magnetic system. Further work on Fe_7S_8 nanowires is ongoing.

Acknowledgment

This work has been supported by the National Natural Science Foundation of China under grant no. 50671087.

References

[1] Yue G H, Yan P X, Liu J Z, Fan X Y and Zhuo R F 2005 *Appl. Phys. Lett.* **87** 262505
[2] Su H L, Ji G B, Tang S L, Li Z, Gu B X and Du Y W 2005 *Nanotechnology* **16** 429
[3] Yue G H, Yan P X, Fan X Y, Wang M X, Qu D M, Yan D and Liu J Z 2006 *J. Appl. Phys.* **100** 124313
[4] Li W, Peng Y, Jones G A, Shen T H and Hill G 2005 *J. Appl. Phys.* **97** 034308
[5] Melle S *et al* 2003 *Appl. Phys. Lett.* **83** 4547
[6] Yue G H, Yan P X, Fan X Y, Wang M X, Qu D M, Wu Z G, Li C and Yan D 2007 *Electrochem. Solid-State Lett.* **10** D29
[7] Hayashi M, Thomas L, Rettner C, Moriya R and Parkin S S P 2007 *Nat. Phys.* **3** 21
[8] Wang H X, Wu Y C, Zhang L D and Hu X Y 2006 *Appl. Phys. Lett.* **89** 232508
[9] Liu S H, Tok J B H, Locklin J and Bao Z N 2006 *Small* **2** 1448
[10] Meister S, Peng H L, McIlwrath K, Jarausch K, Zhang X F and Cui Y 2006 *Nano Lett.* **6** 1514
[11] Zhan Q F, He W, Ma X, Kou Z Q, Di N L and Cheng Z H 2004 *Appl. Phys. Lett.* **85** 4690
[12] Ge S H, Li C, Ma X, Li W, Xi L and Li C X 2001 *J. Appl. Phys.* **90** 509
[13] Cordente N, Respaud M, Senocq F, Casanove M J, Amiens C and Chaudret B 2001 *Nano Lett.* **1** 565
[14] Wang Y W, Zhang L D, Meng G W, Wang Y W, Zhang L D and Meng G W 2002 *J. Phys. Chem.* B **106** 2502
[15] Nath M and Rao C N R 2001 *J. Am. Chem. Soc.* **123** 4841
[16] Xia Y, Gates B, Yin Y, Kim F and Yan H 2003 *Adv. Mater.* **15** 353
[17] Hirahara E and Murakami M 1958 *Phys. Chem. Solids* **7** 281
[18] Li F and Franzen H F 1996 *J. Solid State Chem.* **126** 108
[19] Yang X O, Tsai T Y, Chen D H, Militzer H C, Vogl E M and Rampf F A 2003 *Chem. Commun.* **6** 2210
[20] Sato K 1966 *J. Phys. Soc. Japan* **21** 733
[21] O'Reilly W, Hoffmann V, Chouker A C, Soffel H C and Menyeh A 2000 *Geophys. J. Int.* **142** 669
[22] Harada T 1998 *J. Phys. Soc. Japan* **67** 1352
[23] Foutana M, Bormioli M and Arondo B 1998 *J. Non-Cryst. Solids* **231** 234
[24] Xie Y, Zhu L, Jiang X, Lu J, Zheng X, He W and Li Y 2001 *Chem. Mater.* **13** 3927
[25] Nath M, Choudhury A, Kundu A and Rao C N R 2003 *Adv. Mater.* **15** 2098
[26] Bouchard R J 1968 *J. Cryst. Growth* **2** 40
[27] Pickardt J, Reuter B, Riedel E and Sochtig J 1975 *J. Solid State Chem.* **15** 366
[28] Kong X H, Lou T J and Li Y D 2005 *J. Alloys Compounds* **390** 236
[29] Jeandey C, Oddou J L, Mattei J L and Fillion G 1991 *Solid State Commun.* **78** 195
[30] Gosselin J R, Townsend M G, Tremblay R J and Webster A H 1975 *Mater. Sci. Bull.* **10** 41
[31] Hayase K, Otsuka R and Mariko T 1963 *Mineral. J.* **4** 41
[32] Powell A V *et al* 2004 *Phys. Rev.* B **70** 014415